Geophysical Journal International

Geophys. J. Int. (2021) **225,** 657–663
Advance Access publication 2020 December 29
GJI Seismology

doi: 10.1093/gji/ggaa610

Apparent earthquake rupture predictability

Men-Andrin Meier [1], Jean-Paul Ampuero [2], Elizabeth Cochran [3] and Morgan Page[3]

[1] *Seismological Laboratory, California Institute of Technology, Pasadena, CA 91125, USA. E-mail: mmeier@caltech.edu*
[2] *Observatoire de la Côte d'Azur, Université Côte d'Azur, IRD, CNRS, Géoazur, 06560 Valbonne, France*
[3] *U.S. Geological Survey, Earthquake Science Center, Pasadena, CA 91106, USA*

Received 2020 December 4; in original form 2020 September 15

SUMMARY

To what extent can the future evolution of an ongoing earthquake rupture be predicted? This question of fundamental scientific and practical importance has recently been addressed by studies of teleseismic source time functions (STFs) but reaching contrasting conclusions. One study concludes that the initial portion of STFs is the same regardless of magnitude. Another study concludes that the rate at which earthquakes grow increases systematically and strongly with final event magnitudes. Here, we show that the latter reported trend is caused by a selection bias towards events with unusually long durations and by estimates of STF growth made when the STF is already decaying. If these invalid estimates are left out, the trend is no longer present, except during the first few seconds of the smallest events in the data set, M_w 5–6.5, for which the reliability of the STF amplitudes is questionable. Simple synthetic tests show that the observations are consistent with statistically indistinguishable growth of smaller and larger earthquakes. A much weaker trend is apparent among events of comparable duration, but we argue that its significance is not resolvable by the current data. Finally, we propose a nomenclature to facilitate further discussions of earthquake rupture predictability and determinism.

Key words: Earthquake dynamics; Earthquake early warning; Earthquake interaction, forecasting, and prediction; Earthquake source observations.

1 INTRODUCTION

Whether earthquakes of all sizes start the same is a fundamental question for earthquake source physics, with practical implications for earthquake early warning (EEW) systems. For decades, a set of studies have argued that it is possible to distinguish between small and large earthquakes early in the rupture process (e.g. Ellsworth & Beroza 1995; Beroza & Ellsworth 1996; Colombelli *et al.* 2014; Melgar & Hayes 2019). Earthquakes that differ early in their rupture process require earthquake evolutions that are not self-similar, such as nucleation processes that scale with final magnitude size (Ellsworth & Beroza 1995; Beroza & Ellsworth 1996) or development of a strong slip pulse (Melgar & Hayes 2019). However, similar numbers of studies instead assert that small and large earthquakes are indistinguishable at their start (e.g. Mori & Kanamori 1996; Meier 2016; Ide 2019; Trugman *et al.* 2019). This view, often referred to as the cascade model (Ellsworth & Beroza 1995), posits that earthquakes begin similarly, but some grow to larger sizes as a consequence of favourable conditions for continued slip (e.g. friction, stress distribution, geometry, etc.; Abercrombie & Mori 1994; Kilb & Gomberg 1999).

Short-time predictability of earthquake rupture, if real and systematic, could be exploited to accelerate alerts provided by EEW systems. If estimates of the final expected magnitude could be made well before the rupture was complete, using, for example, the first few seconds of the observed *P* wave, then warnings could rapidly be provided to the entire region expected to experience potentially damaging ground shaking (Olson & Allen 2005; Allen & Melgar 2019; Colombelli *et al.* 2020). If instead EEW systems had to observe a large fraction of the final rupture extent to estimate the magnitude, warnings could be delayed relative to the more optimistic case by a few to tens of seconds or longer for the very largest events (Minson *et al.* 2018; Trugman *et al.* 2019).

One way to address the question of whether the early evolution of large to great quakes differs is to examine the growth rates of source time functions (STFs), which quantify the temporal evolution of slip velocity integrated across the rupture surface (Tanioka & Ruff 1997). STFs are among the source properties most robustly constrained by teleseismic data and are thus available for a large number of earthquakes worldwide (Vallée & Douet 2016). This work analyses some pitfalls of studies of earthquake rupture predictability based on STFs.

Despite the robustness of STFs, two studies based on them recently conducted by Meier *et al.* (2017, hereafter 'MA17') and Melgar & Hayes (2019, hereafter 'MH19') have reached contradictory conclusions. Both studies analysed large databases of STFs,

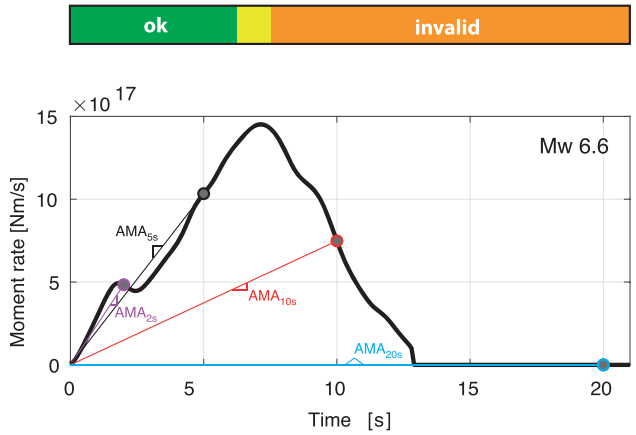

Figure 1. Measurement of AMA as defined by MH19 at 2, 5, 10 and 20 s on the STF of an M6.6 earthquake. The measurements at 10 and 20 s do not represent the growth rate of this earthquake because the STF is already decaying or over (i.e. for AMA_{20s}, the slope is equal to zero), respectively.

each derived with a consistent method (Vallée *et al.* 2011; Ye *et al.* 2016; Hayes 2017). MA17 find that early STF growth rates of large ($M_w > 7$) subduction thrust earthquakes do not vary with magnitude. In contrast, MH19 report that larger earthquakes accelerate much faster than smaller ones: their analysis suggests that an M_w8.0 earthquake accelerates an order of magnitude faster than an M_w7.0 earthquake. The motivation of this work is to understand the origin of this discrepancy and to develop nomenclature to facilitate further discussions of earthquake rupture predictability.

2 MEASURING RUPTURE GROWTH

The rupture onsets of earthquakes of different magnitudes can be compared by direct inspection of their STFs. Because STFs have large fluctuations that are highly variable among events of a same magnitude, MA17 compared the median STFs of various magnitude bins. The conclusion of their basic analysis, supported by statistical testing, is that the onsets of large ($M_w > 7$) subduction thrust earthquakes are independent of magnitude.

Rupture onsets can also be quantified by a measure of the initial growth rate of STFs. MH19 measured the 'average moment acceleration' (AMA) in four time intervals (2, 5, 10 and 20 s) by dividing the moment rate at the end of the interval by the interval duration T_m. Raw plots of AMA as a function of magnitude, as in fig. 2 of MH19, do show a strong correlation, which MH19 interpreted as indicative of rupture predictability. Even their AMA measurements made at 2 s after origin time show a visible correlation with final event magnitudes, spanning more than an order of magnitude, although MH19 do not deem this correlation significant.

As illustrated in Fig. 1, AMA is a meaningful measure of moment growth while the STF is still in the growing phase. However, after the STF has reached its peak, AMA no longer represents the growth phase of the earthquake.

Since a majority of the events in the data set used by MH19 ['optimal' STFs from the SCARDEC database (Vallée *et al.* 2011), considering all hypocentral depths and source mechanisms] have magnitudes between 5.5 and 7.0, the measurement windows of 2, 5, 10 and 20 s are relatively long compared to the source duration for most events. Fig. 2 shows the STF durations for the same data set. We determined the typical source duration for each magnitude, $T_{typical}(m)$, with an ordinary least-squares fit assuming a linear relation between the logarithm of duration and magnitude (black line). The data points are coloured according to the duration ratio $r_T = T_{obs}/T_{typical}$, where T_{obs} is the observed source duration of an individual STF. Here, we define T_{obs} as twice the centroid durations of the STF (Duputel *et al.* 2013), but different definitions do not change our conclusions. The largest quakes may have longer rupture durations than predicted due to the finite width of the seismogenic zone (e.g. Scholz 1982; Shimazaki 1986; Romanowicz 1992). Thus, we may underestimate the average duration of the largest quakes, as may be suggested in Fig. 2 for magnitudes greater than $\sim M$7.5 where more events have higher duration ratios.

If STFs are roughly symmetric (Tanioka & Ruff 1997; Houston 2001), AMA measurements should be made at times shorter than half of the source duration to ensure that the measurement is made before the peak moment rate. The typical rupture duration of, for example, a magnitude 6.5 earthquake is $\sim$<10 s (Fig. 2). For the events with below-average durations, AMA measurements made later than $T_{typical}/2 \sim 5$ s will be made after the STF peak, and so they will underestimate the true AMA the STF had while it was growing (Fig. 1).

To avoid this, one could selectively use only AMA measurements from STFs that had not yet reached their peak at the time of measurement. But this introduces a second artefact, a selection bias: if we measure AMA at 5 s for all M6.5 events that have not yet reached their STF peak at this point in time, we preferentially select events that have above-average STF durations (red colours in Fig. 2). Most of the STFs with below-average durations (blue colours in Fig. 2) will already have reached the STF peak and the selection procedure excludes them.

This selection bias directly bears on the AMA measurements. Moment rates and source durations are linked in that, for a given seismic moment, the higher the moment rate, the faster the final seismic moment is reached, i.e. the shorter the source duration. Preferentially selecting events with atypically long source durations therefore implies selecting events with atypically low moment rates.

We suggest that the main results of MH19 are a consequence of the two artefacts described above: underestimates of STF growth made during STF decay and a selection bias towards events with unusually long durations. To illustrate this, we use the same data set as MH19 and reproduce their fig. 2 with two primary modifications (Fig. 3). AMA measurements made after the peak moment rate are plotted as small black dots. They are not valid quantifications of moment-rate growth and will be largely ignored in the remainder of this comment. The remaining AMA measurements are coloured according to duration ratio r_T as in Fig. 2.

This colour scheme reveals that the main trend of strongly growing AMA with M_w in Fig. 3 is indeed caused by the two artefacts. The low AMA values for small magnitudes are either from STFs that are already past their peak (black dots) or they have atypically long durations (high r_T, warm colours). For a given seismic moment, long durations imply low moment-rate amplitudes and correspondingly low AMA. Likewise, the events with the highest AMA measurements are mostly events with atypically short durations (cool colours). For events with typical durations (yellow), a slight trend between AMA and magnitude remains but is much weaker than the order-of-magnitude trend suggested by MH19: its slope is about half the apparent slope of the whole data set. In Section 4, we examine whether or not this secondary trend is real.

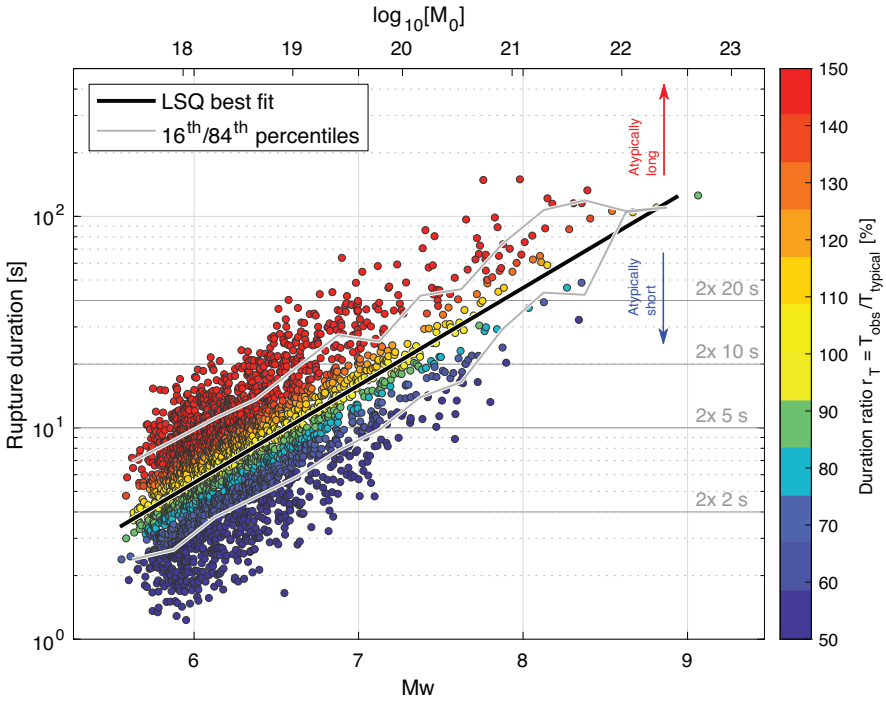

Figure 2. STF durations versus moment magnitudes, coloured with the duration ratio $r_T = T_{obs}/T_{typical}$ to show events with above- and below-average durations. Black line is an ordinary least-squares best fit, such that $\log_{10}M_o = 0.308(\log_{10}T_{typical}) - 4.8375$. Grey lines give the 16th and 84th percentiles in narrow magnitude bins. Horizontal grey lines give the minimum source duration to make a valid AMA measurement if STFs are roughly symmetric.

3 SYNTHETIC STFS WITH MAGNITUDE-INDEPENDENT GROWTH RATES

We further confirm that the main trend is a result of the selection bias by modelling simple, synthetic STFs with magnitude-independent onsets (Figs 4a and b). We draw 3000 magnitudes from a truncated Gutenberg–Richter distribution for M_w between 6.0 and 9.0, and compute rupture durations using

$$T = cM_0{}^{1/3} \times 10^{N(0,0.026)},$$

where $c = 4.93 \times 10^{-6}$ has been optimized to match the observed durations in the data set with a fixed exponent of 1/3. The log-normal random perturbations (N) were selected to approximately match the variability of the observed durations (0.026). We use the STF model of (Juhel *et al.* 2018), based on self-similar circular crack models, to construct STFs with quadratic growth, and that reach their peak moment rate at half duration. For a given seismic moment M_0 and duration T, the growing half of the STF is

$$\dot{M}_0(t) = a\frac{M_0}{T/2}\left(\frac{t}{T/2}\right)^2 \quad \text{for } 0 < t \le T/2.$$

For the decaying half, the model is a polynomial approximation to the stopping phase of the Madariaga 1976 circular crack model:

$$\dot{M}_0(t) = a\frac{M_0}{T/2}\left(1 - \left(\frac{t}{T/2} - 1\right)^2\right)^6, \quad \text{for } T/2 < t \le T.$$

The coefficient $a = 1.483$ is such that the integral of the STF is M_0.

Together, the quadratic growth and the $T \propto M_0{}^{1/3}$ scaling result in synthetic STFs with magnitude-independent onsets. That is, larger or smaller magnitudes grow at the same rate on average, until they reach the peak rate and start decaying. The AMA at time T_m is $\dot{M}_0(T_m)/T_m = 2a\frac{M_0}{(T/2)^3}T_m$. For earthquakes with typical duration, $T \approx T_{typical} \propto M_0^{1/3}$, the AMA follows $\dot{M}_0(T_m)/T_m \propto T_m$; thus, it is independent of M_0. Similarly, for any STF model with power-law onset $\dot{M}_0(t) \propto (M_0/T)/(t/T)^p$, the AMA is $\dot{M}_0(T_m)/T_m \propto (M_0/T^{p+1})T_m^{p-1}$. If the STF onset is magnitude-independent, its moment and duration satisfy $M_0 \propto T^{p+1}$ and the AMA is independent of moment.

Despite this magnitude independence, these simple synthetic STFs lead to the same apparent trend as the real STFs (Figs 4a and b). This shows that the main trend in Figs 2(a)–(d) and discussed by MH19 is an apparent one, caused by the two aforementioned issues. We also observe the same trends if we compute synthetics that grow linearly rather than quadratically (not shown), which may be a more appropriate model for the largest $M_w > 7.0$ earthquakes (MA17). The selection bias necessarily arises when we measure the STF properties at discrete time intervals, unless the time intervals are much shorter than the source durations.

The distinct log-linear upper envelope of the AMA trend with M_0 has the form AMA$<\sim M_0/T_m^2$. MH19 qualitatively interpret this linear scaling to reflect a self-similar pulse model. However, the envelope trend has a trivial explanation. On the one hand, from dimensional analysis it follows that AMA $\propto M_0/T_{obs}^2$ if $M_0 \propto T_{obs}^3$ (Kanamori & Anderson 1975). On the other hand, non-zero AMA measurements have to be made at times shorter than the source duration, $T_m < T_{obs}$. Thus, AMA $<\sim M_0/T_m^2$. In other words, unless an STF had an erratic shape, its M_0 and T put an upper bound on

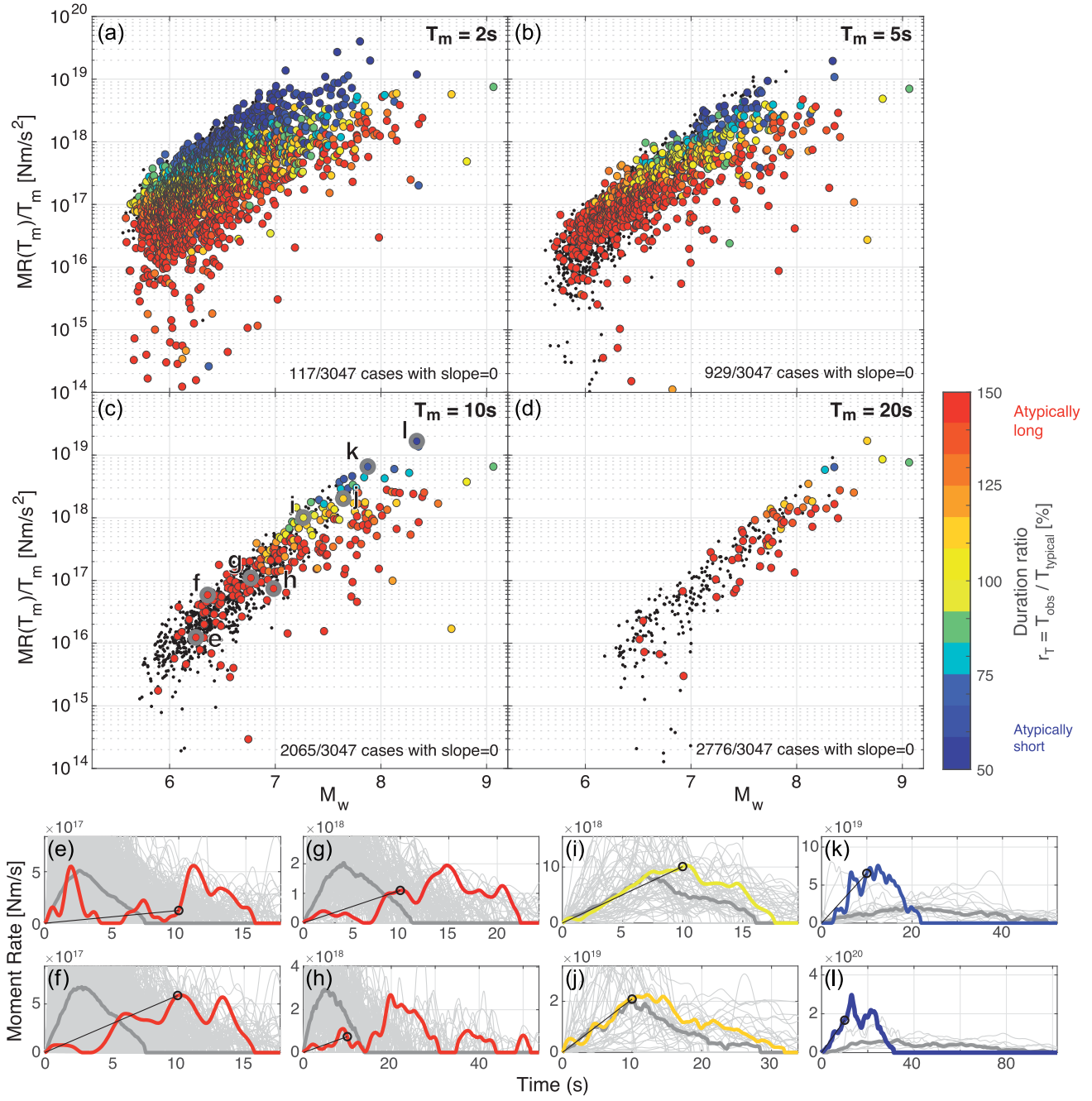

Figure 3. (a–d) Observed AMA at 2, 5, 10 and 20 s as a function of magnitude. This is the same as MH19's fig. 2 but with colour showing if an event is unusually long (red) or short (blue), given its magnitude. AMAs of STFs that have already passed their peak moment rate are shown as black dots. In each panel, we list the number of events where the measured slope (AMA) is equal to zero. Panels (e)–(l) show example STFs labelled in (c) (bold lines coloured by duration ratio) compared to all STFs of the same magnitude ±0.1 units (thin grey lines) and their median (thick grey line).

the rate at which it can grow. If it had an AMA above the observed envelope, it would reach its final moment M_0 at a time that is shorter than the measurement interval T_m.

The lower envelope of the AMA data also has an approximate log-linear trend. In the synthetic case, this lower envelope trend is a consequence of the Gutenberg–Richter distribution of magnitudes: it disappears if we assume instead a uniform magnitude–frequency distribution. The larger number of AMA $<$ 1e16 Nm s^{-2} measurements in the synthetic STFs results from their gradual termination. The real STFs tend to terminate more abruptly.

4 DOES THE SECONDARY TREND SUGGEST RUPTURE PREDICTABILITY?

The above considerations show that the first-order trend discussed by MH19 is an artefact. We also noted in Fig. 3, a much weaker trend between AMA and magnitude among events with similar relative duration (symbols of same colour). The more difficult question is whether this secondary trend is real. If we only look at observed STFs with durations that lie within 80 and 120 per cent of the typical duration (yellow colours in Fig. 3), we qualitatively observe

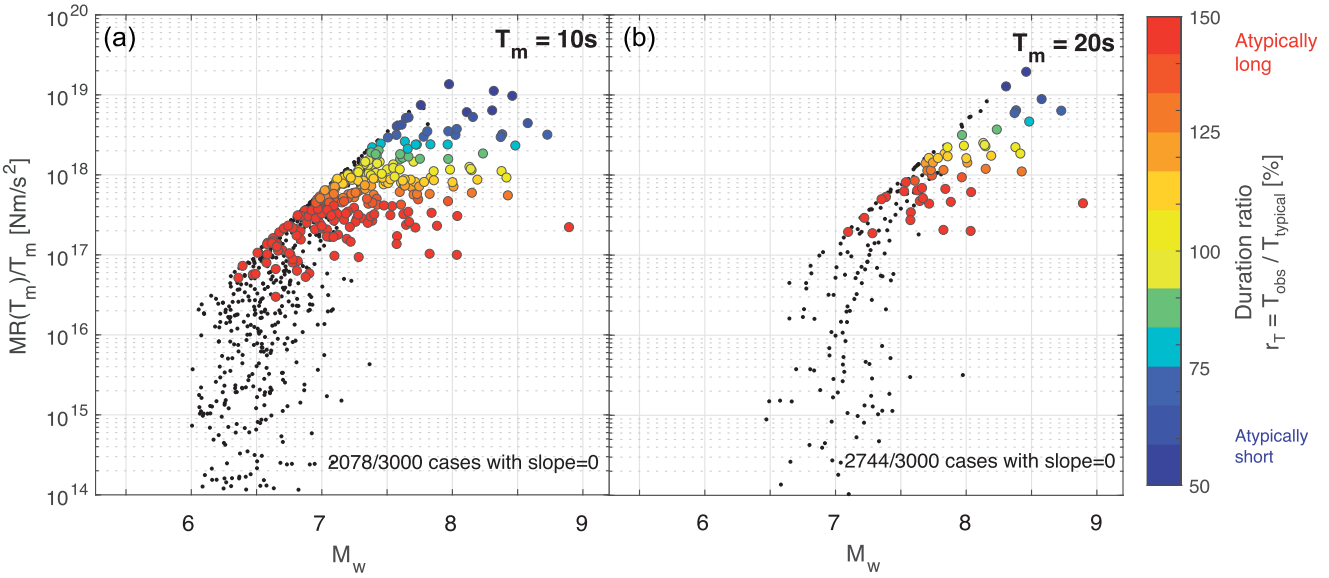

Figure 4. (a and b) The same as Figs 3(c) and (d) for a synthetic data set of quadratically growing STFs with magnitude-independent growth rates.

a correlation between M_w and $\log_{10}$(AMA); however, this trend is not present in the synthetic data (Figs 4a and b).

For the largest time window (20 s), unbiased AMA estimates are possible for only a few of the largest magnitude events, nine of which have typical durations according to the above criterion. It is plausible that these largest events at some point develop extraordinary moment rate accelerations that are reached only by the very largest earthquakes (*cf.* fig. S7 in MA17). But, while the hypothesis is plausible, the small number of data does not allow a convincing test. The largest events may also be expected to have more obvious finite-fault effects that may cause trade-offs between space and time in the STFs (e.g. Ihmlé 1998), although Vallée *et al.* (2011) took steps to reduce these trade-offs. Finally, our estimate of the $T_{typical}$ assumes $M_0 \propto T_{obs}^3$ that may cause the durations of largest quakes to be underestimated, as discussed above and suggested in Fig. 2. This underestimate could result in an apparent trend between M_w and $\log_{10}$(AMA) for $M >\sim 7.5$, such as that observed in Fig. 3(d).

In the 10 s window, where more unbiased estimates are available (47 events with typical durations), and where the STFs should be relatively well resolved, minimal correlation is observed. For the two shortest time windows, notable correlations are observed. At such short time windows, however, the reliability of the teleseismic STF amplitudes is questionable. MA17 reported that their smallest magnitude bin ($M_w \sim 7.0$) had lower STF slopes than the other bins, but they attributed the trend to resolution artefacts from the teleseismic source inversions. There are various reasons for why early STF amplitudes may be affected by resolution artefacts, including: (i) phase-arrival-time uncertainties of ± 2 s (Vallée *et al.* 2011), (ii) magnitude-dependent bandpass filters that are applied before the STF inversion for $M_w < 7.0$ events (Vallée & Douet 2016), (iii) the depletion of high frequencies in teleseismic records which may have a stronger relative effect on smaller than on larger magnitude events and (iv) the fact that, in least-squares inversions, early low-amplitude values can be affected by later high-amplitude values. In the SCARDEC data set, even the very first STF samples (at 0.07 s) qualitatively correlate with final magnitude (Fig. 5), and the observed trend resembles that in Fig. 2. This suggests that early STF amplitudes may indeed be affected by resolution artefacts. Therefore, more research is needed to establish how reliably teleseismic

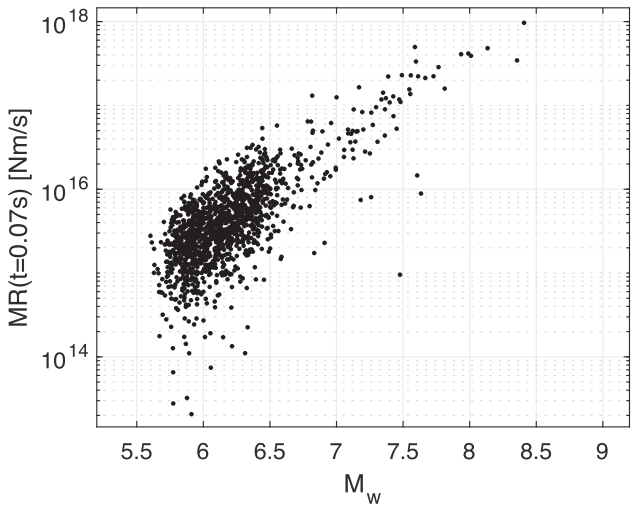

Figure 5. Amplitudes of first samples of SCARDEC STFs at $t = 0.07$ s versus final moment magnitudes. The apparent correlation between the initial STF amplitudes and final moment magnitude highlights that STFs must be carefully verified before being used to derive information about the early evolution of earthquakes. The main text lists several reasons why early STF amplitudes may be affected by resolution artefacts.

STFs can resolve event onsets and the temporal evolution of smaller ($M_w <\sim 7.0$) events.

In summary, convincing correlations between AMA and final event magnitudes are observed only for a small number of very large magnitude events, and for short time windows, where the accuracy of the STF amplitudes is unknown. This may suggest that even this weaker, secondary trend is an artefact, rather than evidence for rupture predictability. Notably, other, more direct lines of evidence that do not suffer from the same limitations show no difference in rupture growth rates for at least several seconds after the onset. This includes peak displacement observations from short-distance seismograms (Meier *et al.* 2016), peak displacement records from local distance ranges (Noda & Ellsworth 2016; Trugman *et al.* 2019) and seismogeodetic waveforms (Goldberg *et al.* 2019).

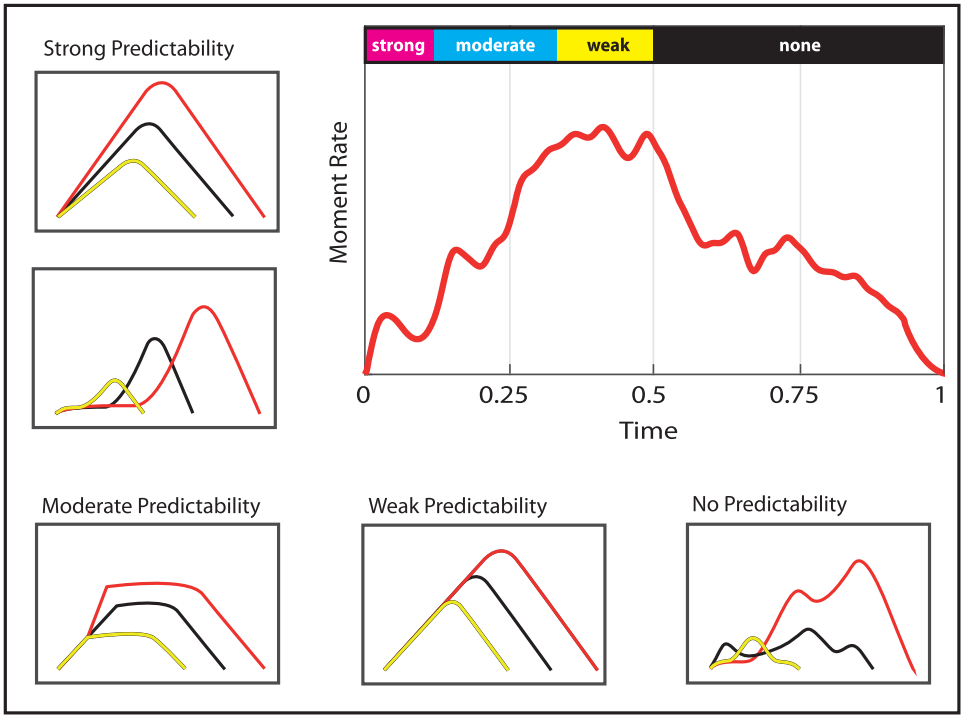

Figure 6. Conceptual models for rupture predictability. How soon into the rupture can final magnitudes be estimated accurately? In models with 'strong' rupture predictability, smaller and larger ruptures can already be distinguished at <10 per cent of the full rupture duration of the smaller events of the comparison, for example, because larger ruptures start more impulsively (e.g. Nakatani *et al.* 2000) or less impulsively (Ellsworth & Beroza 1995; Beroza & Ellsworth 1996; Colombelli *et al.* 2014). In models with 'moderate' predictability, smaller and larger ruptures have statistically indistinguishable onsets, but develop magnitude-dependent properties between one-tenth and one-third of their full rupture duration (e.g. Melgar & Hayes, 2017, 2019; Danré *et al.* 2019). In models with 'weak' rupture predictability, accurate magnitude estimates are possible between one-third and half of the full rupture duration (Meier *et al.* 2017; Trugman *et al.* 2019).

5 A NOMENCLATURE FOR RUPTURE PREDICTABILITY

In models with magnitude-independent rupture growth, smaller and larger earthquakes start to differ significantly once the smaller one has reached its peak moment rate. This is what MA17 described as 'weak rupture predictability' because, in this case, one does not have to wait until the rupture is terminated to make accurate estimates of the final rupture size. Accurate estimates are possible as soon as the peak moment rate is reached, which MA17 found to occur between 35 and 55 per cent of the full rupture duration, for events with $M_w \geq 7$. At around the same time, MH17 used a similar term, 'weak determinism', to describe a somewhat different model, in which rupture growth properties are independent of final magnitudes only in the first few seconds of the rupture. Then, after 'approximately tens of seconds' the rupture organizes into a self-similar pulse with kinematic properties that depend on final event magnitudes.

In order to have a consistent nomenclature to describe rupture predictability and determinism phenomena, we propose the following convention, in which predictability statements are expressed with respect to the full rupture duration (Fig. 6). In models with 'strong predictability', accurate magnitude estimates can be made based on observations that span <10 per cent of the full rupture duration (Ellsworth & Beroza 1995; Beroza & Ellsworth 1996; Nakatani *et al.* 2000; Olson & Allen 2005; Colombelli *et al.* 2014). 'Weak predictability' means that accurate estimates are possible at one-third to half of the rupture duration, that is, towards the end of the growth phase of the rupture (MA17; Trugman *et al.* 2019). 'Moderate predictability' describes the intermediate case when accurate estimates are possible before one-third of the rupture is complete, but not as early as at <10 per cent of the full duration (MH19; Danré *et al.* 2019). 'No predictability' describes the case when accurate estimates are possible only after the rupture is complete. Such a convention may prevent misunderstandings in future predictability and determinism arguments.

Typical rupture durations for *M*5.0, 6.0, 7.0 and 8.0 earthquakes are 1, 4, 12 and 40 s, respectively (Fig. 2; Hanks & Thatcher 1972). If an *M*7.0 earthquake can be distinguished from an *M*8.0 earthquake after 10 s, this does not imply strong, moderate or even weak rupture predictability because at this point the *M*7.0 is already close to over. If, on the other hand, we can distinguish an *M*8.0 from an *M*9.0 at 10 s, this would imply moderate predictability because 10 s is only about 25 per cent of the rupture duration of the *M*8.0 earthquake.

The current debate mostly revolves around whether rupture predictability is moderate (Danré *et al.* 2019) or weak (Trugman *et al.* 2019). The studies reporting evidence for strong predictability are mostly from a time when data availability and quality were inferior compared to today (Ellsworth & Beroza 1995; Beroza & Ellsworth 1996; Olson & Allen 2005; Colombelli *et al.* 2014). At face value, the observations of MH19 suggest strong rupture predictability (visible correlation of AMA with M_w already at 2 s), though in the text they argue only for moderate predictability. Our analysis suggests

that their inference is dominated by artefacts. It is entirely plausible that there is some trend between early rupture growth rates and final magnitudes. However, given the body of literature on the question, this trend would have to be relatively weak, much weaker than the order-of-magnitude trend suggested by MH19.

6 CONCLUSIONS

To measure and compare earthquake growth rates, we need to consider the natural statistics of earthquake populations (large variability in rupture durations, Gutenberg–Richter frequency magnitude distribution), as well as the resolution limits of earthquake source inference methods. For the magnitude ranges where teleseismic STFs permit meaningful moment-rate growth measurements, STFs are consistent with magnitude-independent rupture growth and with weak rupture predictability. That is, smaller and larger earthquakes grow with the same average rates and can only be distinguished once the smaller earthquakes have reached their peak moment rate.

DATA AVAILABILITY

The STFs used in this study from Valle´e *et al.* (2011) can be downloaded from http://scardec.projects.sismo.ipgp.fr/(last accessed in November 2020). This research was partially funded by U.S. Geological Survey Cooperative Agreement G19AC00296 and the Gordon and Betty Moore Foundation Grant 5229 to Caltech.

REFERENCES

Abercrombie, R. & Mori, J., 1994. Local observations of the onset of a large earthquake: 28 June 1992 Landers, California, *Bull. seism. Soc. Am.,* **84,** 725–734.

Allen, R.M. & Melgar, D., 2019. Earthquake early warning: advances, scientific challenges, and societal needs, *Annu. Rev. Earth Planet. Sci.,* **47,** 361–388.

Beroza, G.C. & Ellsworth, W.L., 1996. Properties of the seismic nucleation phase. Seismic source parameters: from microearthquakes to large events, *Tectonophysics,* **261,** 209–227.

Colombelli, S., Festa, G. & Zollo, A., 2020. Early rupture signals predict the final earthquake size, *Geophys. J. Int.,* **223,** 692–706.

Colombelli, S., Zollo, A., Festa, G. & Picozzi, M., 2014. Evidence for a difference in rupture initiation between small and large earthquakes, *Nat. Commun.,* **5,** 3958. doi:10.1038/ncomms4958.

Danré, P., Yin, J., Lipovsky, B.P. & Denolle, M.A., 2019. Earthquakes within earthquakes: patterns in rupture complexity, *Geophys. Res. Lett.,* **46,** 7352–7360.

Duputel, Z., Tsai, V.C., Rivera, L. & Kanamori, H., 2013. Using centroid time-delays to characterize source durations and identify earthquakes with unique characteristics, *Earth planet. Sci. Lett.,* **374,** 92–100.

Ellsworth, W.L. & Beroza, G.C., 1995. Seismic evidence for an earthquake nucleation phase, *Science,* **268,** 851–855.

Goldberg, D.E., Melgar, D. & Bock, Y., 2019. Seismogeodetic *P*-wave amplitude: no evidence for strong determinism, *Geophys. Res. Lett.,* 2019GL083624, doi:10.1029/2019GL083624.

Hanks, T.C. & Thatcher, W., 1972. A graphical representation of seismic source parameters, *J. geophys. Res.,* **77,** 4393–4405.

Hayes, G.P., 2017. The finite, kinematic rupture properties of great-sized earthquakes since 1990, *Earth planet. Sci. Lett.,* **468,** 94–100.

Houston, H., 2001. Influence of depth, focal mechanism, and tectonic setting on the shape and duration of earthquake source time functions, *J. geophys. Res.,* **106,** 11137–11150.

Ide, S., 2019. Frequent observations of identical onsets of large and small earthquakes, *Nature,* **573,** 112–116.

Ihmlé, P.F., 1998. On the interpretation of subevents in teleseismic waveforms: the 1994 Bolivia deep earthquake revisited, *J. geophys. Res.,* **103**(B8), 17 919–17 932.

Juhel, K. *et al.*, 2018. Earthquake early warning using future generation gravity strainmeters, *J. geophys. Res.,* **123,** 10 889–10 902.

Kanamori, H. & Anderson, D.L., 1975. Theoretical basis of some empirical relations in seismology, *Bull. Seism. Soc. Am.,* **65,** 1073–1095.

Kilb, D. & Gomberg, J., 1999. The initial subevent of the 1994 Northridge, California, earthquake: is earthquake size predictable?, *J. Seismol.,* **3,** 409–420.

Meier, M.-A., Ampuero, J.P. & Heaton, T.H., 2017. The hidden simplicity of subduction megathrust earthquakes, *Science,* **357,** 1277–1281.

Meier, M.A., Heaton, T. & Clinton, J., 2016. Evidence for universal earthquake rupture initiation behavior, *Geophys. Res. Lett.,* **43**(15), 7991–7996.

Melgar, D. & Hayes, G.P., 2017. Systematic observations of the slip pulse properties of large earthquake ruptures: slip pulse properties of earthquakes, *Geophys. Res. Lett.,* **44,** 9691–9698.

Melgar, D. & Hayes, G.P., 2019. Characterizing large earthquakes before rupture is complete, *Sci. Adv.,* **5,** eaav2032. doi:10.1126/sciadv.aav2032.

Minson, S.E., Meier, M.-A., Baltay, A.S., Hanks, T.C. & Cochran, E.S., 2018. The limits of earthquake early warning: timeliness of ground motion estimates, *Sci. Adv.,* **4,** eaaq0504. doi:10.1126/sciadv.aaq0504.

Mori, J.J. & Kanamori, H., 1996. Initial rupture of earthquakes in the 1995 Ridgecrest, California sequence, *Geophys. Res. Lett.,* **23,** 2437–2440.

Nakatani, M., Kaneshima, S. & Fukao, Y., 2000. Size-dependent microearthquake initiation inferred from high-gain and low-noise observations at Nikko district, Japan, *J. geophys. Res.,* **105,** 28 095–28 109.

Noda, S. & Ellsworth, W.L., 2016. Scaling relation between earthquake magnitude and the departure time from *P* wave similar growth, *Geophys. Res. Lett.,* **43,** 9053–9060.

Olson, E.L. & Allen, R.M., 2005. The deterministic nature of earthquake rupture, *Nature,* **438,** 212–215.

Romanowicz, B., 1992. Strike-slip earthquakes on quasi-vertical transcurrent faults: inferences for general scaling relations, *Geophys. Res. Lett.,* **19,** 481–484.

Scholz, C.H., 1982. Scaling laws for large earthquakes; consequences for physical models, *Bull. seism. Soc. Am.,* **72,** 1–14.

Shimazaki, K., 1986. Small and large earthquakes; the effects of the thickness of seismogenic layer and the free surface, *Geophys. Monogr. Ser.,* **37,** 209–216.

Tanioka, Y. & Ruff, L.J., 1997. Source time functions, *Seismol. Res. Lett.,* **68,** 386–400.

Trugman, D.T., Page, M.T., Minson, S.E. & Cochran, E.S., 2019. Peak ground displacement saturates exactly when expected: implications for earthquake early warning, *J. geophys. Res.,* **124,** 4642–4653.

Vallée, M., Charléty, J., Ferreira, A.M.G., Delouis, B. & Vergoz, J., 2011. SCARDEC: a new technique for the rapid determination of seismic moment magnitude, focal mechanism and source time functions for large earthquakes using body-wave deconvolution: wave deconvolution and earthquake parameters, *Geophys. J. Int.,* **184,** 338–358.

Vallée, M. & Douet, V., 2016. A new database of source time functions (STFs) extracted from the SCARDEC method, *Phys. Earth planet. Inter.,* **257,** 149–157.

Ye, L., Lay, T., Kanamori, H. & Rivera, L., 2016. Rupture characteristics of major and great ($M_w \geq 7.0$) megathrust earthquakes from 1990 to 2015: 1. Source parameter scaling relationships, *J. geophys. Res.,* **121,** 826–844.